The C_{32} alkane-1,15-diol as a proxy of late Quaternary riverine input in coastal margins

Julie Lattaud[1*], Denise Dorhout[1], Hartmut Schulz[2], Isla S. Castañeda[1,5], Enno Schefuß[3], Jaap S. Sinninghe Damsté[1,4], Stefan Schouten[1,4]

[1]*NIOZ Royal Netherlands Institute for Sea Research, Department of Marine Microbiology and Biogeochemistry, and Utrecht University, PO Box 59, 1790 AB Den Burg, The Netherlands*

[2] *University of Tübingen, Department of Geosciences, Hölderlinstrasse 12, D-72074 Tübingen, Germany*

[3]*MARUM Center for Marine Environmental Sciences, University of Bremen, Germany.*

[4]*Utrecht University, Department of Earth Sciences, Faculty of Geosciences, Budapestlaan 4, 3584 CD Utrecht, The Netherlands.*

[5] *Present address: University of Massachusetts, Department of Geological sciences, 244 Morrill Science Center, Amherst, United States of America*

**Corresponding author: Julie.lattaud@nioz.nl*

To be resubmitted to Climate of the Past

ABSTRACT

The study of past sedimentary records from coastal margins allows us to reconstruct variations of terrestrial input into the marine realm and to gain insight into continental climatic variability. There are numerous organic proxies for tracing terrestrial input into marine environments but none that strictly reflect the input of river-produced organic matter. Here, we test the fractional abundance of the C_{32} alkane 1,15-diol relative to all 1,13- and 1,15-long-chain diols ($F_{C32\ 1,15}$) as a tracer of input of river-produced organic matter in the marine realm in surface and Quaternary (0-45 ka) sediments on the shelf off the Zambezi and nearby smaller rivers in the Mozambique Channel (western Indian Ocean). A Quaternary (0-22 ka) sediment record off the Nile River mouth in the Eastern Mediterranean was also studied for long-chain diols. For the Mozambique Channel, surface sediments of sites most proximal to Mozambique Rivers showed the highest $F_{1,15\text{-}C32}$ (up to 10%). The sedimentary record shows high (15-35%) pre-Holocene $F_{1,15\text{-}C32}$ and low (<10%) Holocene $F_{1,15\text{-}C32}$ values, with a major decrease between 18 and 12 ka. $F_{1,15\text{-}C32}$ is significantly correlated (r^2=0.83, p<0.001) with the BIT index, a proxy for the input of soil and river-produced organic matter in the marine environment, which declines from 0.25-0.60 for the pre-Holocene to <0.10 for the Holocene. This decrease of both $F_{C32\ 1,15}$ and the BIT is interpreted to be mainly due to rising sea level, which caused the Zambezi River mouth to become more distal to our study site, thereby decreasing riverine input at the core location. Some small discrepancies are observed between the records of the BIT index and $F_{C32\ 1,15}$ for Heinrich Event 1 (H1) and Younger Dryas (YD), which may be explained by a change in soil sources in the catchment area rather than a change in river influx. Like for the Mozambique Channel, a significant correlation between $F_{C32\ 1,15}$ and the BIT index (r^2=0.38, p<0.001) is

observed for the Eastern Mediterranean Nile record. Here also, the BIT index and $F_{C32\ 1,15}$ are lower in the Holocene than in the pre-Holocene, which is likely due to the sea level rise. In general, the differences between BIT index and $F_{C32\ 1,15}$ Eastern Mediterranean Nile records can be explained by the fact that the BIT index is not only affected by riverine runoff but also by vegetation cover with increasing cover leading to lower soil erosion. Our results confirm that $F_{C32\ 1,15}$ is a complementary proxy for tracing riverine input of organic matter into marine shelf settings and, in comparison with other proxies, it seems not to be affected by soil and vegetation changes in the catchment area.

1. Introduction

Freshwater discharge from river basins into the ocean has an important influence on the dynamics of many coastal regions. Terrestrial organic matter (OM) input by fluvial and aeolian transport represents a large source of OM to the ocean (Schlesinger and Melack, 1981). Deltaic and marine sediments close to the outflow of large rivers form a sink of terrestrial OM and integrate a history of river, catchment, and oceanic variability (Hedges et al, 1997).

Terrestrial OM can be differentiated from marine OM using carbon to nitrogen (C/N) ratios and the bulk carbon isotopic composition (^{13}C) of sedimentary OM (e.g. Meyers, 1994). The abundance of N-free macromolecules such as lignin or cellulose result in organic carbon-rich plant tissues that lead to an overall higher C/N ratio for terrestrial OM compared to aquatic organisms (Hedges et al., 1986). However, this ratio may be biased when plant-tissues gain nitrogen during bacterial degradation and when planktonic OM preferentially lose nitrogen over carbon during decay (Hedges and Oades, 1997). Differences in the stable carbon isotopic composition may also be used to examine terrestrial input as terrestrial OM is typically depleted in ^{13}C ($\delta^{13}C$ of -28 to -25‰) compared to marine OM (-22 to -19‰). However, C_4 plants have $\delta^{13}C$ values of around -12‰ (Fry et Sherr, 1984; Collister et al. 1994; Rommerskirchen et al., 2006) and thus a substantial C_4 plant contribution can make it difficult to estimate the proportion of terrestrial to marine OM in certain settings (Goñi et al., 1997).

Biomarkers of terrestrial higher plants are also used to trace terrestrial OM input into marine sediments. For example, plant leaf waxes such as long-chain *n*-alkanes are transported and preserved in sediments (Eglinton and Eglinton 2008, and references cited therein) and can provide information on catchment-integrated vegetation or precipitation changes (e.g. Ponton et al., 2014), while soil specific bacteriohopanepolyols (BHP) are biomarkers of soil bacteria and indicate changes in soil OM transport (Cooke et al., 2008). Similarly, branched glycerol dialkyl glycerol tetraethers (brGDGTs) are widespread and abundant in soils (Weijers et al., 2007, 2009) and can be used to trace soil OM input into marine settings via the branched and isoprenoid tetraether (BIT) Index (Hopmans et al., 2004). However, brGDGTs can also be produced in-situ in rivers (e.g. De Jonge et al., 2015) and thus the BIT index does not exclusively reflect soil OM input. Moreover, because the BIT index is the ratio of brGDGTs to crenarchaeol (an isoprenoidal GDGT predominantly produced by marine Thaumarchaeota; Sinninghe Damsté et al., 2002), the BIT index can also reflect changes in marine OM productivity instead of changes in terrestrial OM input in areas where primary productivity is highly variable, i.e. where the quantity of crenarchaeol is variable (Smith et al., 2012).

Although these terrestrial organic proxies are useful to trace soil, river or vegetation input into marine sediments, previously there were no organic geochemical proxies to specifically trace river-produced OM input. However, recently, the C_{32} 1,15-diol, relative to all 1,13- and 1,15-long-chain diols ($F_{C32\ 1,15}$), was proposed as a tracer for river-produced OM input (De Bar et al., 2016; Lattaud et al., 2017). Long-chain diols (LCD), such as the C_{32} 1,15-diol, are molecules composed of a long alkyl chain ranging from 26 to 34 carbon atoms, an alcohol group at position C_1 and at a mid-chain position, mainly at positions 13, 14 and 15. They occur ubiquitously in marine environments (de Leeuw et al., 1979; Versteegh et al., 1997, 2000; Gogou and Stephanou, 2004; Rampen et al., 2012, 2014; Romero-Viana et al., 2012; Plancq et al., 2015; Zhang et al., 2011 and references therein), where the major diols are generally the C_{30} 1,15-diol,

C_{28} and C_{30} 1,13-diols, and the C_{28} and C_{30} 1,14-diols. In marine environments the 1,14-diols are produced mainly by *Proboscia* diatoms (Sinninghe Damsté et al., 2003; Rampen et al., 2007) and the 1,13 and 1,15-diol are thought to be produced by eustigmatophyte algae (Volkman et al., 1999; Rampen et al., 2007, 2014b; Villanueva et al., 2014). Versteegh et al. (2000) showed that $F_{C32\ 1,15}$ was relatively higher closer to the mouth of the Congo River. Likewise, Rampen et al. (2012) observed that sediments from the estuarine Hudson Bay have a much higher $F_{C32\ 1,15}$ than open-marine sediments. More recent studies noted elevated amounts of $F_{C32\ 1,15}$ in coastal sediments, and even higher amounts in rivers indicating a continental source for this diol (De Bar et al., 2016; Lattaud et al., 2017). Since the C_{32} 1,15-diol was not detected in soils distributed worldwide, production of this diol in rivers by freshwater eustigmatophytes is the most likely source of this compound which, therefore, can potentially be used as a proxy of river-produced OM input to marine settings.

Here we test the downcore application of this new proxy by analyzing $F_{C32\ 1,15}$ in a continental shelf record (0-45 ka) from the Mozambique Channel and a record (0-24 ka) from the Eastern Mediterranean Sea to reconstruct Holocene/Late Pleistocene changes in freshwater input of the Zambezi and Nile rivers, respectively. Analysis of surface sediments and comparison with previously published BIT index records (Castañeda et al., 2010; Kasper et al., 2015) allow us to assess the potential of the C_{32} 1,15-diol as a tracer for riverine runoff, or more precisely, river-produced organic matter, in these coastal margins.

2. Material and Methods

2.1. Study sites

2.1.1. Mozambique margin and Zambezi River

The Mozambique Channel is located between the coasts of Mozambique and Madagascar between 11°S and 24°S and plays an important role in the global oceanic circulation by transporting warm Indian Ocean surface waters into the Atlantic Ocean. The Zambezi River is the largest river that delivers freshwater and suspended particulate matter to the Mozambique Channel (Walford et al., 2005). The Zambezi River has a drainage area of 1.4 x 10^6 km^2 and an annual runoff between 50 and 220 km^3 (Fekete et al., 1999). It originates in northern Zambia, flows through eastern Angola and Mozambique to reach the Indian Ocean. The Zambezi delta starts at Mopeia (Ronco et al., 2006) and the Zambezi plume enters the Mozambique Channel and flows northwards along the coast (Nehama and Reason, 2014). The rainy season in the catchment is in austral summer when the Intertropical convergence zone (ITCZ) is at its southernmost position (Beilfuss and Santos, 2001; Gimeno et al., 2010; Nicholson et al., 2009). The seasonal variation of the Zambezi runoff varies between 7000 m^3/s during the wet season to 2000 m^3/s during the dry season (Beilfuss and Santos, 2001). A few smaller Mozambique rivers other than the Zambezi River flow into the Mozambique Channel (Figure 1): the Ligonha, Licungo, Pungwe and Revue in Mozambique (together with the Zambezi River, they are collectively called “the Mozambique rivers” here).

Past studies have shown that the deposition pattern of the Zambezi riverine detritus is variable with sea level, i.e. most of the time material was deposited downstream of the river mouth but during high sea level it was deposited northeast of the river mouth due to a shore current (Schulz et al., 2011). During the last glacial period the Zambezi riverine detritus followed a more channelized path (Schulz et al., 2011). Van der Lubbe et al. (2016) found that the relative influence of the Zambezi river compared to more northern rivers in the Mozambique Channel varied during Heinrich event 1 (H1) and the Younger Dryas (YD). Schefuß et al. (2011) studied the $\delta^{13}C$ and δD of *n*-alkanes, and the elemental composition (Fe content) of core GeoB9307-3, located close to the present day river mouth (Fig. 1), and reported higher precipitation and riverine terrestrial input in the Mozambique Channel during the Younger Dryas and H1. This is in agreement with more recent results from Just et al. (2014) on core GeoB9307-3 and Wang et al. (2013a) on core GIK16160-3, further away from the actual river mouth; both studies also showed an increased riverine terrestrial input during H1 and YD. To summarize, during H1 and the YD, the Zambezi catchment is characterized by higher precipitation and enhanced riverine runoff due to a southward shift of the Intertropical Convergence Zone (ITZC) resulting from Northern Hemisphere cold events, whereas during the Holocene drier conditions prevailed (Schefuß et al., 2011; Wang et al., 2013; van der Lubbe et al., 2014; Weldeab et al., 2014). The Last Glacial Maximum (LGM) in the Zambezi catchment is also recognized as an extremely wet period (Wang et al., 2013).

2.1.2 Eastern Mediterranean Sea and Nile River

The Eastern Mediterranean Sea is influenced by the input of the Nile River, which is the main riverine sediment supply with annual runoff of 91 km^3 and a sediment load of about 60 x 10^9 $kg.yr^{-1}$ (Foucault and Stanley, 1989; Weldeab et al., 2002). Offshore Israel, the Saharan aeolian sediment supply is very low (Weldeab et al., 2002). A strong north-eastern current distributes the Nile River sediment along the Israeli coast toward our study site. The Nile River consists of two main branches: the Blue Nile (sourced at Lake Tana, Ethiopia) and the White Nile (sourced at Lake Victoria, Tanzania, Uganda). Precipitation in the Nile catchment fluctuates widely with latitude with the area north of 18°N dry most of the year and the wettest areas at the source of the Blue Nile and White Nile (Camberlin, 2009). This general distribution reflects the latitudinal movement of the ITCZ.

Castañeda et al. (2010) have shown that sea surface temperature (SST) (reconstructed with alkenones and TEX_{86}) at the study site was following Northern Hemisphere climate variations with a cooling during the LGM, H1 and the YD and warming during the early part of the deposition of sapropel 1 (S1). Associated H1 and LGM cooling, extreme aridity in the Nile catchment is observed as inferred from the δD of leaf waxes. In contrast, during the early Holocene S1 deposition, a more humid climate and enhanced Nile River runoff prevailed (Castañeda et al., 2016). Neodymium (ε_{Nd}) and strontium ($^{87}Sr/^{88}Sr$) isotopes (Castañeda et al., 2016; Box et al., 2011, respectively) show a relative increase in the contribution of Blue Nile inputs when the climate is arid (H1, LGM) and an increased contribution of the White Nile inputs when the climate is humid (S1). This change also affects the soil input into the Nile River, as inferred from the distribution of branched GDGTs, with a more arid climate reducing the vegetation in the Ethiopian highlands (source of the Blue Nile) and favoring soil erosion while during a more humid climate, vegetation increasing and soil erosion is less (Krom et al., 2002). To summarize, the climate of the Nile catchment area was colder and drier (Castañeda et al., 2010, 2016) during the YD, H1 and the LGM. The LGM and H1 were extremely arid events with the likely desiccation of the Nile water sources, i.e. Lake Tana and Lake Victoria (Castañeda et al., 2016). To the contrary, the time period during S1 sapropel deposition was warmer and wetter resulting in an enhanced riverine runoff. The late Holocene is characterized by a decrease in precipitation (Blanchet et al., 2014).

2.2. Sampling and processing of the sediments

2.2.1. Mozambique Channel sediments

We analyzed 36 core-top sediments (from multi cores) along a transect from the Mozambique coast to Madagascar coast (LOCO transect, Fallet et al. 2012). The LOCO core-tops have been previously studied by XRF and grain-size analysis (van der Lubbe et al., 2014, 2016) as well as for inorganic ($\delta^{18}O$, Mg/Ca) and organic (TEX_{86}, Uk'_{37}) temperature proxies (Fallet et al., 2012). 25 core-top sediments (from grabs, gravity or trigger-weight corers) retrieved during the R/V Valdivia's Expeditions VA02 (1971) and VA06 (1973) (hereafter called VA; Schulz et al., 2011), comprising a north-south transect paralleling the East African coast, and spanning from 21°S to 15°N (Fig. 1a) were also analyzed. These surface sediments have been studied previously for element content (TOC, TON), isotopic content ($\delta^{18}O$, $\delta^{13}C$) as well as for mineral and fossil (foraminifera) content (Schulz et al., 2011). Piston core 64PE304-80 was obtained from 1329 m water depth during the INATEX cruise by the RV Pelagia in 2009 from a site (18°14.44'S, 37°52.14'E) located on the Mozambique coastal margin, approximately 200 km north of the Zambezi delta (Fig. 1a). The age model of core 64PE304-80 is based on ^{14}C dating of planktonic foraminifera (see supplementary information, van der Lubbe, 2014; Kasper et al., 2015) and by correlation of log (Ti/Ca) data from XRF core scanning with those of nearby core GIK16160-3, which also has an age model based on ^{14}C dating of planktonic foraminifera (see van der Lubbe et al., 2014 for details).

The LOCO sediment core-tops were sliced into 0 - 0.25 and 0.25 - 0.5 cm slices and extracted as described by Fallet et al. (2012). Briefly, ultrasonic extraction was performed (x 4) with a solvent mixture of dichloromethane (DCM)/methanol (MeOH) (2 : 1 v/v). The total lipid extract (TLE) was then run through a Na_2SiO_4 column to remove water. The 25 VA core-tops from the Valdivia's expedition were freeze dried on board and stored at 4 °C. They were extracted via Accelerator Solvent Extractor (ASE) using DCM: MeOH mixture 9:1 (v/v) and a pressure of 1000 psi at 100 °C using three extraction cycles.

We analyzed sediments of core 64PE304-80 for diols using solvent extracts that were previously obtained for determination of the BIT index and δD values of alkenones (Kasper et al., 2015). Briefly, the core was sliced into 2 cm thick slices and the sediments were ASE extracted using the method described above.

For all Mozambique Channel sediments, the total lipid extract (TLEs) were separated through an alumina pipette column into three fractions: apolar (Hexane : DCM, 9:1 v/v), ketone (Hexane : DCM, 1:1 v/v) and polar (DCM : MeOH, 1:1 v/v). The polar fractions, containing the diols and GDGTs, were dissolved into a mixture of 99:1 (v/v) Hexane : Isopropanol and filtered through a 0.45 µm PTFE filters.

2.2.2. Eastern Mediterranean sediment core

Gravity core GeoB 7702-3 was collected during the R/V Meteor cruise M52/2 in 2002 from the slope offshore Israel (31°91.1'N, 34°04.4'E) at 562 m water depth (Pätzold et al., 2003, Castañeda et al., 2010). The chronology of this sedimentary record is based on 15 planktonic foraminiferal ^{14}C AMS dates (for details see Supplementary Information, Castañeda et al., 2010).

The sediments have previously been analyzed for GDGTs, alkenones, δD and $\delta^{13}C$ of leaf wax lipids, and bulk elemental composition (Castañeda et al., 2010, 2016). Sediments were sampled every 5 cm and are 1 cm thick, and previously extracted as described by Castañeda et al. (2010). Briefly, the freeze-dried sediment were ASE extracted and the TLEs were separated using an aluminum oxide column into 3 fractions as described above.

2.3. Analysis of long-chain diols

Diols were analyzed by silylation of the polar fraction with 10 µL N,O-Bis(trimethylsilyl)-trifluoroacetamide (BSTFA) and 10 µL pyridine, heated for 30 min at 60°C and adding 30 µL of ethyl acetate. Diol analysis was performed using a gas chromatograph (Agilent 7990B GC) coupled to a mass spectrometer (Agilent 5977A MSD) (GC-MS) and equipped with a capillary silica column (25 m x 320 µm; 0.12 µm film thickness). The oven temperature regime was as follows: held at 70 °C for 1 min, increased to 130 °C at 20 °C/min, increased to 320 °C at 4 °C/min, held at 320 °C during 25 min. Flow was held constant at 2 mL/min. The MS source temperature was held at 250 °C and the MS quadrupole at 150 °C. The electron impact ionization energy of the source was 70 eV. The diols were quantified using selected ion monitoring (SIM) of ions m/z 299.4 (C_{28} 1,14-diol), 313.4 (C_{28} 1,13-diol, C_{30} 1,15-diol), 327.4 (C_{30} 1,14-diol), and 341.4 (C_{32} 1,15-diol) (Versteegh et al., 1997; Rampen et al., 2012).

The fractional abundance of the C_{32} 1,15-diol is expressed as percentage of the total major diols as follows:

$$F_{C32\ 1,15} = \frac{[C_{32}1,15]}{[C_{28}1,13] + [C_{30}1,13] + [C_{30}1,15] + [C_{32}1,15]} \times 100 \qquad (1)$$

2.4. Analysis of GDGTs

GDGTs in the polar fractions of the extracts of the VA and LOCO core-top sediments were analyzed on an Agilent 1100 series LC/MSD SL following the method described by Hopmans et al. (2016). The BIT index was calculated according to Hopmans et al. (2004). We calculated the #ring tetra as described by Sinninghe Damsté et al. (2016) and the CBT index and soil pH as described by Peterse et al. (2012):

$$\#ring\ tetra = \frac{GDGT\ Ib + 2 \times GDGT\ Ic}{GDGT\ Ia + GDGT\ Ib + GDGT\ Ic} \quad (2)$$

$$CBT = \log\left(\frac{GDGT\ Ib + GDGT\ IIb}{GDGT\ Ia + GDGT\ IIa}\right) \quad (3)$$

$$pH = 7.9 - 1.97 \times CBT \quad (4)$$

3. Results

3.1. Surface sediments of the Mozambique Channel

$F_{C32\ 1,15}$ in surface sediments across the Mozambique Channel varies from 2.3 to 12.5% (Fig. 1d, 1f) with one of the highest value in front of the Zambezi River mouth (10%). The core-tops located in front of other minor northern rivers (Licungo, Ligonha Rivers) are also characterized by values of $F_{1,15\text{-}C32}$ (>7.5%) higher than those further away from the coast (< 5%). The major diol in all Mozambique surface sediments is the C_{30} 1,15-diol (57.5±9.9%) with lower amounts of the C_{30} 1,14-diol (21.1±6.0%) and C_{28} 1,14-diol (13.2±4.9%) (Fig. 1f).

The values for the BIT index in surface sediments across the Mozambique Channel vary from 0.01 to 0.42 (Fig. 1c). BIT values are highest in the most northern region (0.4) and in front of river mouths (0.2-0.3) compared to values found close to the coast of Madagascar (<0.04). Following Sinninghe Damsté (2016), we calculated the #ring tetra (the relative abundance of cyclopentane rings in tetramethylated branched GDGTs) to determine if the brGDGTs are in-situ produced in the surface sediments or derived from the continent. The #ring tetra has an average of 0.39±0.03 with higher values in front of the river mouths (with the highest values close to the Madagascar Rivers) and shows a clear decrease towards the open ocean (Fig. 1d). The low #ring tetra indicate that there is likely limited in-situ sedimentary production of brGDGTs in the sediments of the Mozambique coastal shelf area except for the samples closest to the Madagascar coast where high #ring tetra values and low BIT values indicate in-situ production of brGDGTs. However, for the Mozambique shelf, the brGDGTs are mostly derived from the continent, confirming the use of the BIT index as a tracer for riverine input in this region.

3.2. Holocene and Late Quaternary sediments of the Mozambique Channel and Nile River

In the sediments of the Mozambique Channel core 64PE304-80, $F_{C32\ 1,15}$ shows a wide range; it varies from 2.4 to 47.6% (Fig. 2). Between 44 and 39 ka the values are relatively stable (average of 27.6 ± 4.5%), then they rapidly decline between 39 and 36 ka to 11%. From this point on they gradually increase, reaching 37.4% at 17 ka. $F_{C32\ 1,15}$ is then rapidly decreasing until it reaches the lowest values of the record after 12 ka (average of 4.9 ± 1.4%). Holocene sediments (0-11 ka) show relatively low and constant values of $F_{C32\ 1,15}$ (5± 1.5%), similar to the values found in the surface sediments of the area, i.e. 3.5 ± 1.6% (Figs. 1 and 2d).

The BIT index record (data from Kasper et al., 2015) shows similar changes as that of $F_{C32\ 1,15}$. Between 44 and 39 ka the average BIT value is 0.43±0.06, then the BIT value decreases to 0.36 at 36 ka, followed by an increase until 17 ka to reach a value of 0.6, while the Holocene values are constant and average at 0.1±0.02. The #ring tetra of branched GDGTs is constantly low (average 0.15±0.01; Fig. S1a) between 44 to 15.5 ka, then increases to 0.4 at 8 ka and stays constant until the end of the Holocene (average 0.34±0.03). Overall, these values are low and do not approach the values (0.8-1.0) associated with in-situ production of branched GDGTs in coastal marine sediments (Sinninghe Damsté, 2016). The #ring tetra also shows a negative correlation with the BIT index throughout the record (R^2=0.74, $p<0.05$), indicating that when BIT values are high, #ring tetra is low. Therefore, high BIT values can definitely be associated with terrestrial brGDGT input. If we assume that the in-situ production of brGDGTs in the river (e.g. De Jonge et al., 2015; Zell et al., 2015) is minimal, we can then infer sources of soils from the different catchment areas by reconstructing the soil pH via the CBT index (see equation 3 and 4, Peterse et al., 2012). This showed a constant soil pH (average 6.2±0.1) from 43 to 15 ka followed by a slight increase to 7 at 8 ka and constant (average 6.8±0.08) at the end of Holocene (Fig. S1b).

In Eastern Mediterranean sediment core GeoB 7702-3, $F_{C32\ 1,15}$ ranges from 3.9 to 47.0%. Between 24 and 15 ka the values are slowly decreasing from 41% at 24 ka to 7% at 15 ka. Subsequently, $F_{C32\ 1,15}$ raises sharply until 11.7 ka (44%) followed by a sharp decrease down to 16% at 10 ka. $F_{C32\ 1,15}$ increases again until 7.5 ka up to 30%, followed by a slow decrease in the Late Holocene towards values as low as 6% (Fig. 3a). The BIT index (data from Castañeda et al., 2016) varies in a similar way as $F_{C32\ 1,15}$. It is constant between 24 and 17 ka (average 0.37±0.05), then decreases to 0.13 at 14.5 ka. It subsequently increases between 15.6 and 9 ka, before it decreases after 9 ka and stays constant in the Holocene (average 0.17±0.05). The #ring tetra of the brGDGTs (Fig. S1c) is constant from 24 to 15 ka (0.37±0.05) then shows lower values from 15 to 7 ka (0.29±0.04) and, finally, increases again during the late Holocene (0.40±0.05). The BIT index and #ring tetra do not show a clear negative correlation as observed for the Mozambique core. However, the values of #ring tetra values are well below 0.8-1.0, suggesting that in-situ production of brGDGTs does not play an important role, in line with the depth from which the core was obtained which is well below the zone of 100-300 m where in-situ production is most pronounced (Sinninghe Damsté, 2016). During parts of the record, low #ring tetra are associated with high BIT values, indicating that between 24 and 7 ka the brGDGT are mainly terrigenous. For the oldest part of the core, the soil pH shows a stable period from 24 to 14.8 ka (average 6.94±0.07) then increases to 7.3 at 15 ka, followed by a large decrease (pH reaching 6.5 at 8.5 ka). As the in-situ production of brGDGT is likely to be minimal in the latest part of the Holocene, and assuming that riverine production of brGDGTs is minimal, the soil pH can be reconstructed via the CBT index and shows a stable pH (average of 6.8±0.1).

4. Discussion

4.1. Application of C_{32} 1,15-diol as a proxy for riverine input in the Mozambique shelf.

In the surface sediments of the Mozambique Channel $F_{C32\ 1,15}$ is relatively low overall (<10%) in comparison with other coastal regions with substantial river input (Fig. 1f), where values can be as high as 65% (De Bar et al., 2016; Lattaud et al., 2017). Moreover, the BIT values are also relatively low at 0.01-0.42. Further confirmation of the low amount of terrestrial input in the analyzed surface sediments comes from the low C/N values (between 4.2 and 8.9 for the VA surface sediments; Schulz et al., 2011), characteristic of low terrestrial OM input (Meyers 1994). Nevertheless, the slightly higher values of both the BIT index and the $F_{C32\ 1,15}$ near the river mouths indicate that both proxies do seem to trace present day riverine input into the Mozambique Channel in line with earlier findings of other coastal margins influenced by river systems (De Bar et al, 2016; Lattaud et al., 2017).

4.2. Past variations in riverine input in the Mozambique Channel

We compared the record of $F_{C32\ 1,15}$ with previously published proxy records, in particular the BIT index (Kasper et al., 2015) and log (Ca/Ti) (van der Lubbe et al., 2016). These two proxies show the same pattern as $F_{C32\ 1,15}$ (Fig. 2). Indeed, the BIT index and $F_{C32\ 1,15}$ are strongly correlated (r^2 =0.83, $p<0.001$). Since the #ring tetra of brGDGTs varies between 0.06 and 0.4 (Supplementary fig. S1a), and is significantly negatively correlated with the BIT values, the brGDGTs are predominantly derived from the continent (cf. Sinninghe Damsté, 2016) and thus the BIT is likely reflecting riverine input in the marine environment. Furthermore, $F_{C32\ 1,15}$ also shows a significant negative correlation with log(Ca/Ti) (r^2=0.43, $p<0.0001$, van der Lubbe et al., 2016). This is another proxy for riverine input since Ti is mainly derived from erosion of continental rocks transported to the ocean through rivers, whereas Ca derives predominantly from the marine environment.

The records of $F_{C32\ 1,15}$ and BIT index show three major variations: a steep drop from 19 to 10 ka, a slow increase from 38 to 21 ka during the Last Glacial and a steep decrease between 40 to 38 ka. The largest change in the BIT index and $F_{C32\ 1,15}$ is between 19 to 10 ka, i.e. a major drop which coincides with an interval of rapid sea level rise (Fig. 2b). Following Menot et al. (2006), we explain the drop in the BIT index, and consequently also the drop in $F_{C32\ 1,15}$, by the significant sea level rise occurring during this period. Rising sea level flooded the Mozambique plateau, moving the river mouth further away from the core site and establishing more open-marine conditions. This most likely resulted in lower $F_{C32\ 1,15}$ and BIT values, conditions that remained throughout the Holocene. The decrease in the delivery of terrestrial matter is also seen in element ratios (Fe/Ca) and organic proxies (BIT) in nearby core GeoB9307-3 (Schefuß et al, 2011), which is located closer to the present day river mouth in the Mozambique plateau (Fig. 1a). Likewise, the gradual increase in the BIT index and $F_{C32\ 1,15}$ between 38 and 21 ka occurred at a time when sea-level was decreasing (Fig 2b., Grant et al., 2014; Rohling et al., 2014) and thus the river mouth came closer to our study site. The decrease of BIT values and $F_{C32\ 1,15}$ during 40-38 ka coincides with Heinrich event 4 (H4), a cold and dry event in this part of Africa (Partridge et al., 1997; Tierney et al., 2008; Thomas et al., 2009), with dry conditions likely leading to a reduced riverine input into the ocean and thus a reduced input of brGDGTs and the C_{32} 1,15-diol.

Interestingly, there are two periods where BIT and $F_{C32\ 1,15}$ records diverge (Fig. 2a): during the Younger Dryas (YD; 12.7-11.6 ka) and Heinrich event 1 (H1; 17-14.6 ka) with the BIT index decreasing ca. 1 ky later than $F_{C32\ 1,15}$. Comparison with the Ca/Ti ratio shows that both during H1 and the YD, the Ca/Ti ratio increased at the same time as the C_{32} 1,15-diol but earlier than the BIT index, suggesting that the latter was influenced by other parameters. The BIT index is the ratio of brGDGTs (produced mostly in soil or in-situ in rivers in this area based on the low values for #ring tetra; Sinninghe Damsté, 2016) over crenarchaeol (produced mainly in marine environment; Schouten et al., 2013 and references cited therein). As both the Ti/Ca ratio and $F_{C32\ 1,15}$ indicate a decrease in riverine input, a constant BIT index can be explained by two options: a simultaneous decrease in crenarchaeol (marine) production or a change in soil input with higher brGDGT concentrations eroding into the river. The concentration of crenarchaeol during H1 is relatively stable but there is a slight decrease of crenarchaeol during YD (Fig. S2b). Thus, the difference between BIT and $F_{C32\ 1,15}$ during YD can be partly explained by decreased crenarchaeol production together with a decrease in branched GDGTs due to a reduced river flow leading to relatively stable BIT values. In contrast, crenarchaeol and brGDGT concentrations are relatively stable during H1 and thus the lower river input, as indicated by the Ca/Ti and $F_{C32\ 1,15}$, apparently did not lead to a decrease in brGDGT input. This could be due to a shift of sources of soil which are eroded in the river, i.e. if in this period there is a shift towards soils with relatively higher brGDGT concentrations, the BIT index would remain high despite decreased river flow.

A shift in soil sources may be due to two major changes that happened during this period (and also during the YD), i.e. a shift in catchment area of the Zambezi River (Schefuß et al., 2011; Just et al., 2014) and a shift in the relative influence of the Zambezi River versus northern Mozambique rivers (van der Lubbe et al., 2016). The shift in catchment area is evident from the higher influx of kaolinite-poor soil into the marine system during H1 and YD (Just et al., 2014) coming from the Cover Sands of the coastal Mozambique area (Fig. 3d, blue circle), relative to the kaolinite-rich soils of the hinterlands (Fig. 3d, red circles). If the brGDGT concentrations from the latter region are higher, then this change of soil input could lead to a stable brGDGT flux into the marine environment, despite decreasing Zambezi River runoff. Support for a shift in soil sources comes from the soil pH record reconstructed from brGDGTs, which during the YD shows a shift towards more acidic soils. However, no change in soil pH are observed during H1.

The relative influence of other rivers (Lurio, Rovuma Rivers) relative to the Zambezi River (Fig. 3d green circle) was inferred from neodymium isotopes by Van der Lubbe et al. (2016), i.e. more radiogenic rocks are found in the northern river catchments in comparison to the rocks in the Zambezi catchment (Fig. 2b). These authors found that during H1 and YD, the relative contribution of the northern rivers is lower than normal, likely due to drought conditions north of the Zambezi catchment area (Tierney et al., 2008, 2011; Just et al., 2014). These northern rivers run through a catchment containing mainly humid highstand soils, which are different soil types than observed in the catchment area of the Zambezi River (van der Lubbe et al., 2016). We hypothesize that higher brGDGT concentrations in the soils of the catchment areas of the Zambezi River can potentially explain the discrepancy between BIT and $F_{C32\ 1,15}$, i.e. during H1 and YD there is more input of brGDGT-rich soils from the Zambezi than brGDGT-poor soils from the northern rivers leading to constant BIT values despite a dropping riverine input. Further research examining the brGDGT contents of soils in the different river catchment areas as well as surface sediments from offshore these northern rivers is required to distinguish between the different hypotheses.

4.3. Past variations in riverine input in the Eastern Mediterranean Sea

With the Eastern Mediterranean Sea core, we compared $F_{C32\ 1,15}$ in core GeoB7702 with other proxies including the BIT index, log (Ca/Ti) and strontium isotopes, the latter to infer the relative importance of the Blue Nile and the White Nile as source regions (Fig. 4c-e). The BIT values (data from Castañeda et al., 2010) show a significant positive correlation with $F_{C32\ 1,15}$ (r^2=0.38, $p < 0.05$), while log (Ca/Ti) shows an negative correlation to $F_{C32\ 1,15}$, again supporting a continental origin of the C_{32} 1,15-diol. $F_{C32\ 1,15}$ and BIT records show much lower Holocene values (12±6%) compared to pre-Holocene (27±11%), which again can be attributed to the sea level rise occurring during the last deglaciation, i.e. our study site was further away from the river mouth and the amount of continental-derived OM reaching the site decreased. Both records show low values during H1 comparable to the Holocene. These low values can be attributed to extreme aridity in the Nile River catchment (Castañeda et al., 2016), which we hypothesize led to a lack of vegetation and enhanced soil erosion but also leading to a severely reduced river flow, thereby decreasing the net amount of river borne OM reaching our core site.

In this core, there are 3 major discrepancies observed between the BIT index and $F_{C32\ 1,15}$: (1) during the LGM, between 22-19 ka, where the C_{32} 1,15-diol shows a decrease while the BIT index remains constant, (2) during the onset of the deposition of S1 (6.1-10.5 ka, Grant et al., 2016) where the BIT index decreases later than the C_{32} 1,15-diol, and (3) after 2 ka when the BIT index increases while the C_{32} 1,15-diol decreases. For the LGM $F_{C32\ 1,15}$ is decreasing, log (Ca/Ti) is as well, but the BIT index remains constant (and the brGDGT concentration is also low; see supplementary figure S3) indicating that there is no significant decrease in terrigenous OM reaching the core site at that time. During the LGM, there is no significant change in continental climate, based on the findings of Castañeda et al. (2016), suggesting no change in vegetation cover or river flux. This suggests that the change in $F_{C32\ 1,15}$ is not due to a change in the input of C_{32} 1,15-diol but in other, mainly marine derived, diols, in particular the C_{30} 1,15-diol. If this hypothesis is true then an increase in this marine diol will lower the $F_{C32\ 1,15}$ but if the amount of crenarchaeol is not changing at the same time, the BIT values will remain unaffected.

The deposition of S1 is described as a period of increased freshwater input leading to stratification and anoxia (Rossignol-Strick et al., 1982). However, an increased river input is neither reflected in $F_{C32\ 1,15}$ nor in the BIT index, in fact both of them are asynchronously decreasing. Castañeda et al. (2010) showed that the decrease in the BIT index is due to a large increase in crenarchaeol (Supplementary figure S3), much larger than the increase in brGDGTs, due to increased productivity and preservation. A similar scenario may apply for the diols, i.e. the marine diols (in particular the C_{30} 1,15-diol, data not shown) are also increasing at that time more substantially than the C_{32} 1,15-diol, thus lowering $F_{C32\ 1,15}$. However, there is a difference in timing, i.e. the BIT index decreases slightly later than the C_{32} 1,15-diol (9.1 and 10.5 ka, respectively). The decrease in $F_{C32\ 1,15}$ coincides with a substantial increase in sea level (Fig. 4b), which would cause the distance between the core site and the river mouth to increase, thereby decreasing the amount of terrigenous material reaching the site. This terrigenous decrease is also visible to some extent in the log (Ca/Ti) but not in the BIT index. Possibly, like with the Mozambique Channel, the brGDGT concentrations in the river were much higher at that time. Indeed, the Sr isotopic record suggest a major shift from a Blue Nile to a White Nile source at 10.5 ka, with the latter possibly containing more eroded soils with high brGDGT concentrations. This shift in soil sources is also shown in the change towards more acidic soil pH during that period based on the CBT index (Supplementary figure S1d).

For the most recent part of the record (0-5 ka), the BIT index increases, while $F_{C32\ 1,15}$ is slightly decreasing. The $\delta D_{leaf\ waxes}$ (Fig 4.d) shows it was period of mild aridity which likely led to a decreased riverine runoff and thus decreased river input. The reason the BIT index is increasing rather than decreasing is due to an increase in brGDGT concentrations (Fig. 3b), despite evidence for a decrease in river runoff. This can possibly be linked to the amount of vegetation in the Nile catchment, i.e. at that time there was a decrease in vegetation cover (Blanchet et al., 2014; Castañeda et al., 2016), which led to more soil erosion and thus potentially a higher brGDGT concentration in rivers and a higher BIT index. This hypothesis is supported by the log (Ca/Ti) (Fig. 4c), which is decreasing at this time, suggesting that soil runoff was increasing.

Our results from both the Nile and Mozambique Channel cores illustrate that $F_{C32\ 1,15}$ provides a suitable proxy for reconstructing past riverine input into coastal seas. Although some discrepancies are noted with other terrigenous proxies for both cores, $F_{C32\ 1,15}$ generally agrees well with these proxies. However, our interpretation of the C_{32} 1,15-diol record relies on the assumption that production of this diol in rivers is not changing with different hydroclimate fluctuations on land, something that needs to be tested. However, De Bar et al. (2016) showed that $F_{C32\ 1,15}$ in the Tagus River in Portugal did not significantly change over the course of a year, suggesting that this assumption might be valid. Since the C_{32} 1,15-diol is mainly produced in rivers itself, it is not impacted by vegetation abundance and soil composition, in contrast to other proxies like the BIT index and lignin concentrations. This may make it a potentially more reliable proxy to trace past river input into marine environments.

6. Conclusion

We studied core-tops in the Mozambique Channel and two sediment cores, in the Mozambique Channel, off the Zambezi River mouth and in the Eastern Mediterranean Sea, offshore the Nile delta, to test $F_{C32\ 1,15}$ as a proxy for riverine input into the marine realm. The surface sediments show that the C_{32} 1,15-diol traces present day riverine input into the Mozambique Channel, supported by the BIT index. In both sediment records, $F_{C32\ 1,15}$ is significantly correlated with the BIT index showing the applicability of this proxy to trace riverine input, but also showed some discrepancies. This can be explained by the different sources of these proxies, i.e. the BIT index is reflecting soil and river-produced OM input and the C_{32} 1,15-diol is mainly reflecting river-produced OM input. Our multiproxy approach suggests that the timing of changes in the different terrestrial proxies records can differ due to changes in catchment area or to shifting importance of the different source rivers.

Author contribution

S. S. and J. L. designed the study. J. Lattaud analyzed the surface sediments for diols and GDGTs and core GeoB 7702-3 for diols, I. C. sampled and extracted the surface sediments and the sediment cores 64PE304-80 and GeoB 7702-3, D. D. analyzed the sediment core 64PE304-80 for diols. H. S. collected the VA core-tops, E.S. collected core GeoB7702-3. J. L., S. S., I. C. and J.S.S.D. interpreted the data. J. L. wrote the manuscript with input of all authors.

The authors declare that they have no conflict of interest.

Acknowledgement

We thank Anchelique Mets and Jort Ossebaar for analytical help. This research has been funded by the European Research Council (ERC) under the European Union's Seventh Framework Program (FP7/2007-2013) ERC grant agreement [339206] to S.S. J.S.S.D. and S.S. received financial support from the Netherlands Earth System Science Centre and this work was in part carried out under the program of the Netherlands Earth System Science Centre (NESSC), financially supported by the Ministry of Education, Culture and Science (OCW). Sample material of core GeoB7702-3 has been provided by the GeoB Core Repository at the MARUM – Center for Marine Environmental Sciences, University of Bremen, Germany. The data reported in this paper are archived in Pangaea (www.pangaea.de).

References

Beilfuss, R. and Santos, D.: Patterns of hydrological change in the Zambezi delta. Mozambique (Working Paper No. 2, International Crane Foundation, Sofala, Mozambique, 2001), 1–89, 2001.

Blanchet, C.L., Frank, M. and Schouten, S.: Asynchronous changes in vegetation, runoff and erosion in the Nile River watershed during the Holocene, 2014, PLoS ONE 9(12): e115958. doi:10.1371/journal.pone.0115958.

Box, M.R., Krom, M.D., Cliff, R.A., Bar-Matthews, M., Almogi-Labin, A., Ayalon, A. and Pateme, M.: Response of the Nile and its catchment to millennial-scale climatic change since the LGM from Sr isotopes and major elements of East Mediterranean sediments, Quat. Sci. Rev., 30, 431-442, 2011. doi.org/10.1016/j.quascirev.2010.12.005.

Camberlin, P.: The Nile, chapter Nile basin climate, ed. Springer, 307-333, 2009.

Castañeda, I.S., Schefuß, E., Pätzold, J., Sinninghe Damsté, J.S., Weldeab, S. and Schouten, S. : Millennial-scale sea surface temperature changes in the eastern Mediterranean (Nile River Delta region) over the last 27,000 years, Paleoceanography, 25, 2010. doi:10.1029/2009PA001740.

Castañeda, I.S., Schouten, S., Pätzold, J., Lucassen, F., Kasemann, S., Kuhlmann, H. and Schefuß, E.: Hydroclimate variability in the Nile River Basin during the past 28,000 years, Earth Planet. Sci. Lett., 438, 47-56, 2016. doi.org/10.1016/j.epsl.2015.12.014.

Collister, J.W., Rieley, G., Stern, B., Eglinton, G. and Fry, B.: Compound-specific $\delta^{13}C$ analyses of leaf lipids from plants with differing carbon dioxide metabolisms, Org. Geochem., 21 (6-7), 619-627, 1994. doi.org/10.1016/0146-6380(94)90008-6.

Cooke, M.P., Talbot, H.M. and Wagner, T.: Tracking soil organic carbon transport to continental margin sediments using soil-specific hopanoid biomarkers: A case study from the Congo fan (ODP site 1075), Org. Geochem., 39 (8), 965-971, 2008. doi.org/10.1016/j.orggeochem.

De Bar, M., Dorhout, D. J., C., Hopmans, E.C., Sinninghe Damsté, J.S. and Schouten, S. : Constraints on the application of long chain diol proxies in the Iberian Atlantic margin, Org. Geochem., 184-195, 2016. doi/10.1016/j.orggeochem.2016.09.005.

De Jonge, C., Stadnitskaia, A., Hopmans, E.C., Cherkashov, G., Fedotov, A., Streletskaya, I.D., Vasiliev, A.A. and Sinninghe Damsté, J.S.: Drastic changes in the distribution of branched tetraether lipids in suspended matter and sediments from the Yenisei River and Kara Sea (Siberia): Implications for the use of brGDGT-based proxies in coastal marine sediments, Geochimica et Cosmochimica Acta 165 200-225, 2015. doi.org/10.1016/j.gca.2015.05.044.

De Leeuw, J.W., Rijpstra, W.I.C. and Schenck, P.A., The occurrence and identification of C_{30}, C_{31} and C_{32} alkan-1,15-diols and alkan-15-one-1-ols in Unit I and Unit II Black Sea sediments, Geochim. Cosmochim. Acta, 45, 2281-2285, 1981, doi:10.1016/0016-7037(81)90077-6 .

Eglinton, T.I. and Eglinton, G.: Molecular proxies for paleoclimatology, Earth Planet. Sc. Lett., 275, 1-16, 2008. doi/10.1016/j.epsl.2008.07.012.

Fallet, U., Brummer, G.-J., Zinke, J., Vogels, S. and Ridderinkhof, H. : Contrasting seasonal fluxes of planktonic foraminifera and impacts on paleothermometry in the Mozambique Channel upstream of the Agulhas Current, Paleoceanography, 25, 1525-2027, 2010. doi:10.1029/2010PA001942.

Fallet, U., Castañeda, I.S., Henry-Edwards, A., Richter, T.O., Boer, W., Schouten, S. and Brummer, G.-J. : Sedimentation and burial of organic and inorganic temperature proxies in the Mozambique Channel, SW Indian Ocean, Deep Sea Res. Pt1., 59, 37-53, 2012. doi:10.1016/j.dsr.2011.10.002.

Fekete, B. M., Vörösmarty, C. J. and Grabs, W.: Global, Composite runoff fields based on observed river discharge and simulated water balances, Global Biogeochem. Cycles, 16 (3), 15-1–15-10, 1999.

Foucault, A. and Stanley, D.J.: Late Quaternary paleoclimatic oscillations in East Africa recorded by heavy mineral in the Nile delta, Nature, 339, 44-46, 1989. doi:10.1038/339044a0.

Fry, B. and Sherr, E. B.: $\delta^{13}C$ measurements as indicators of carbon flow in marine and freshwater ecosystems, Contributions to Marine Science 27, 13-47, 1984. doi:10.1007/978-1-4612-3498-2_12.

Gimeno, L., Drumond, A., Nieto, R., Trigo, R.M. and Stohl, A.: On the origin of continental precipitation, Geophys. Res. Lett., 37, 2010. doi: 10.1029/2010GL043712.

Gogou, A. and Stephanou, E.G., Marine organic geochemistry of the Eastern Mediterranean: 2. Polar biomarkers in Cretan Sea surficial sediments, Mar. Chem.85, 1-25, 2004, doi: 10.1016/j.marchem.2003.08.005.

Goñi, M.A., Ruttenberg, K.C. and Eglington, T.I. : Sources and contribution of terrigenous organic carbon to surface sediments in the Gulf of Mexico, Nature, 389, 275-278, 1997. doi:10.1038/38477.

Grant, K.M., Rohling, E.J., Ramsey, C.B., Cheng, H., Edwards, R.L., Florindo, F., Heslop, D., Marra, F., Roberts, A.P., Tamisiea, M.E. and Williams, F.: Sea-level variability over five glacial cycles, Nature com., 5, 2014. doi: 10.1038/ncomms6076.

Hedges, J. I., Clark, W. A., Quay, P. D., Richey, J. E., Devol, A. H. and Santos, U. M. : Composition and fluxes of particulate organic material in the Amazon River, Limnology and Oceanography. 31, 717-738, 1986. doi: 10.4319/lo.1986.31.4.0717.

Hedges, J. I. and Oades, J. M.: Comparative organic geochemistries of soils and sediments, Organic Geochemistry. 27, 319–361, 1997. doi.org/10.1016/S0146-6380(97)00056-9.

Hopmans, E.C., Weijers, J.W.H., Schefuß, E., Herfort, L., Sinninghe Damsté, J.S. and Schouten, S.: A novel proxy for terrestrial organic matter in sediments based on branched and isoprenoid tetraether lipids, Earth Planet. Sc. Lett., 224 (1-2), 107-116, 2004. doi.org/10.1016/j.epsl.2004.05.012.

Hopmans, E.C., Schouten, S. and Sinninghe Damsté, J.S.: The effect of improved chromatography on GDGT-based palaeoproxies, Org. Geochem., 93, 1-6, 2016. doi.org/10.1016/j.orggeochem.2015.12.006.

Just, J., Schefuß, E., Kuhlmann, H., Stuut, J.-B. W. and Pätzold, J. : Climate induced sub-basin source-area shifts of Zambezi River sediments over the past 17 ka, Palaeogeogr., Palaeocl., 410, 190-199, 2014. doi.org/10.1016/j.palaeo.2014.05.045.

Kasper, S., van der Meer, M.T.J., Castañeda, I.S., Tjallingii, R., Brummer, G.-J. A., Sinninghe Damsté, J.S. and Schouten, S.: Testing the alkenone D/H ratio as a paleo indicator of sea surface salinity in a coastal ocean margin (Mozambique Channel), Org. Geochem., 78, 62-68, 2015. doi.org/10.1016/j.orggeochem.2014.10.011.

Krom, M.D, Stanley, J.-D., Cliff, R. A., Woodward, J.C.: Nile River sediment fluctuations over the past 7000 yr and their key role in sapropel development, Geology, 30, 71-74, 2002. doi: 10.1130/0091-7613(2002)030<0071.

Lattaud, J., Kim, J.-H., De Jonge, C., Zell, C., Sinninghe Damsté, J.S. and Schouten, S.: The C_{32} alkane-1,15-diol as a tracer for riverine input in coastal seas, Geochim. Cosmochim. Ac., 202C, 146-158, 2017. doi.org/10.1016/j.gca.2016.12.030.

Ménot, G., Bard, E., Rostek, F., Weijers, J.W.H., Hopmans, E.C., Schouten, S. and Sinninghe Damsté, J.S.: Early reactivation of European Rivers during the last deglaciation, Science, 313, 1623-1625, 2006. doi: 10.1126/science.1130511.

Meyers, P. A.: Preservation of elemental and isotopic source identification of sedimentary organic matter, Chem. Geol.114, 289-302, 1994. doi.org/10.1016/0009-2541(94)90059-0.

Nehama, F.P.J. and Reason, C.J.C. : Morphology of the Zambezi River Plume on the Sofala Bank, Mozambique Western Indian Ocean, J. Mar. Sci. 13, 1-10, 2014.

Nicholson, S.E.: A revised picture of the structure of the “monsoon” and land ITCZ over West Africa, Clim. Dynam., 32, 1155-1171-, 2009. doi: 10.1007/s00382-008-0514-3.

Partridge, T.C., Demenocal, P.B., Lorentz, S.A., Paiker, M.J. and Vogel, J.C.: Orbital forcing of climate over South Africa: A 200,000-year rainfall record from the Pretoria saltpan, Quat. Sc. Rev., 16, 1125-1133, 1997. doi:10.1016/S0277-3791(97)00005-X.

Pätzold, J., Bohrmann G., and Hübscher C. : Black Sea–Mediterranean–Red Sea: Cruise No. 52, Meteor-Ber. 03-2, 179., 2003, Univ. Hamburg, Hamburg, Germany, 2 Jan. to 27 March.

Peterse, F., van der Meer, J., Schouten, S., Weijers, J.W.H., Fierer, N., Jackson, R.B., Kim, J.-H. and Sinninghe Damste, J.S.: Revised calibration of the MBT–CBT paleotemperature proxy based on branched tetraether membrane lipids in surface soils, Geochim. Cosmochim. Acta., 96, 215-229, 2012. doi:10.1016/j.gca.2012.08.011.

Plancq, J., Grossi, V., Pittet, B., Huguet, C., Rosell-Melé, A. and Mattioli, E., Multi-proxy constraints on sapropel formation during the late Pliocene of central Mediterranean (southwest Sicily), Earth Planet. Sci. Lett. 420, 30-44, 2015, doi: 10.1016/j.epsl.2015.03.031.

Ponton, C., West, A., Feakins, S.J. and Valier G.: Leaf wax biomarkers in transit record river catchment composition, Geophys. Res. Lett., 41, 6420–6427, 2014.

Rampen, S.W, Schouten, S., Wakeham, S.G. and Sinninghe Damsté, J.S. : Seasonal and spatial variation in the sources and fluxes of long chain diols and mid-chain hydroxy methyl alkanoates in the Arabian Sea, Org. Geochem., 38, 165–179, 2007. doi.org/10.1016/j.orggeochem.2006.10.008.

Rampen, S.W., Willmott, V., Kim, J.-H., Uliana, E., Mollenhauer, G., Schefuß, E., Sinninghe Damsté, J.S. and Schouten, S. : Long chain 1,13- and 1,15-diols as a potential proxy for palaeotemperature reconstruction, Geochim. Cosmochim.Acta 84, 204–216, 2012. doi.org/10.1016/j.gca.2012.01.024.

Rampen, S.W., Datema, M., Rodrigo-Gámiza, M., Schouten, S., Reichart, G.-J. and Sinninghe Damsté, J.S.: Sources and proxy potential of long chain alkyl diols in lacustrine environments, Geochim. Cosmochim. Acta, 144, 59-71, 2014. doi.org/10.1016/j.gca.2014.08.033.

Rohling, E.J., Foster, G.L., Marino, G., Roberts, A.P., Tamisiea, M.E. and Williams, F.: Sea-level and deep-sea-temperature variability over the past 5.3 million years, Nature, 508, 477-482, 2014. doi:10.1038/nature13230.

Romero-Viana, L., Kienel, U. and Sachse, D., Lipid biomarker signatures in a hypersaline lake on Isabel Island (Eastern Pacific) as a proxy for past rainfall anomaly (1942–2006 AD), Palaeogeogr. Palaeoclimatol. Palaeoecol. 350–352, 49–61, 2012, doi: 10.1016/j.palaeo.2012.06.011.

Rommerskirchen, F., Plader, A., Eglinton, G., Chikaraishi, Y. and Rullkötter, J. : Chemotaxonomic significance of distribution and stable carbon isotopic composition of long-chain alkanes and alkan-1-ols in C_4 grass waxes, Org. Geochem., 37, 1303–1332, 2006. doi.org/10.1016/j.orggeochem.2005.12.013.

Ronco, P., Fasolato, G., and Di Silvio, G. : The case of Zambezi River in Mozambique: some investigations on solid transport phenomena downstream Cahora Bassa Dam, Proceeding of International Conference on Fluvial Hydraulics, Riverflow,1345-1354, 2006. doi: 10.1201/9781439833865.ch143.

Rossignol-Strick, M., Nesteroff, W., Olive, P. and Vergnaud-Grazzini, C.: After the deluge: Mediterranean stagnation and sapropel formation, Nature, 295, 105–110, 1982. doi: 10.1038/295105a0.

Schefuß, E., Kuhlmann, H., Mollenhauer, G., Prange, M. and Pätzold, J. : Forcing of wet phases in southeast Africa over the past 17,000 years, Nature 480, 509-512, 2011. doi:10.1038/nature10685.

Schlesinger, L.H. and Melack, J.M.: Transport of organic carbon in the world's rivers Tellus 33 (2) 172-187, 1981. doi.org/10.3402/tellusa.v33i2.10706.

Schouten, S., Hopmans, E.C. and Sinninghe Damsté, J.S.S., The organic geochemistry of glycerol dialkyl glycerol tetraether lipids: A review, Org. Geochem., 54, 19-61, 2013. doi.org/10.1016/j.orggeochem.2012.09.006.

Schulz, H., Lückge, A., Emeis, K.-C. and Mackensen, A. : Variability of Holocene to Late Pleistocene Zambezi riverine sedimentation at the upper slope off the Mozambique, 15-21°S, Mar. Geol., 286, 21-34, 2011. doi:10.1016/j.margeo.2011.05.003.

Sinninghe Damsté, J.S., Schouten, S., Hopmans, E.C., van Duin, A.C.T. and Geenevasen, J.A.J., Crenarchaeol the characteristic core glycerol dibiphytanyl glycerol tetraether membrane lipid of cosmopolitan pelagic crenarchaeota, Jour. Lip. Res., 43, 1641-1651, 2002. doi: 10.1194/jlr.M200148-JLR200.

Sinninghe Damsté, J.S., Rijpstra, W.I.C., Abbas, B., Muyzer, G. and Schouten, S., A diatomaceous origin for long-chain diols and mid-chain hydroxy methyl alkanoates widely occurring in Quaternary marine sediments: indicators for high nutrient conditions, Geochim. Cosmochim. Acta 67, 1339–1348, 2003, doi: 10.1016/S0016-7037(02)01225-5.

Sinninghe Damsté, J.S.: Spatial heterogeneity of sources of branched tetraethers in shelf systems: The geochemistry of tetraethers in the Berau River delta (Kalimantan, Indonesia), Geochim. Cosmochim. Acta. 186, 13-31, 2016. doi.org/10.1016/j.gca.2016.04.033.

Smith, R.W., Bianchi, T.S. and Li, X.: A re-evaluation of the use of branched GDGTs as terrestrial biomarkers: Implications for the BIT Index, Geochim. Cosmochim. Acta, 80, 14-29, 2012. doi.org/10.1016/j.gca.2011.11.025.

Thomas, D.S.G., Bailey, R., Shaw, P.A., Durcan, J.A. and Singarayer, J.S.: Late Quaternary highstands at Lake Chilwa, Malawi: Frequency, timing and possible forcing mechanisms in the last 44 ka, Quat. Sc. Rev., 28, 526-539, 2009. doi:10.1016/j.quascirev.2008.10.023.

Tierney, J. E., Russell J.M., Huang, Y., Sinninghe Damsté, J.S., Hopmans, E.C. and Cohen, A.S.: Northern Hemisphere controls on tropical southeast African climate during the past 60,000 years, Science 322, 252–255, 2008. doi: 10.1126/science.1160485.

Tierney, J.E., Russell, J.M., Sinninghe Damsté, J.S., Huang, Y. and Verschuren, D.: Late Quaternary behavior of the East African monsoon and the importance of the Congo Air Boundary, Quat. Sc. Rev. 30, 798-807, 2011. doi.org/10.1016/j.quascirev.2011.01.017

van der Lubbe, J. J. L., Tjallingii, R., Prins, M. A., Brummer, G.-J. A., Jung, S. J. A., Kroon, D. and Schneider, R. R.: Sedimentation patterns off the Zambezi River over the last 20,000 years, Mar. Geol., 355, 189–201, 2014. doi:10.1016/j.margeo.2014.05.0120025-3227.

van der Lubbe, J.J.L., Frank, M., Tjallingii, R. and Schneider, R.: Neodymium isotope constraints on provenance, dispersal, and climate-driven supply of Zambezi sediments along the Mozambique Margin during the past ∼45,000 years, Geochem. Geophys., 17 (1), 181-198, 2016. doi:10.1002/2015GC006080.

Versteegh, G.J.M., Bosch, H.J. and De Leeuw, J.W. : Potential palaeoenvironmental information of C_{24} to C_{36} mid-chain diols, keto-ols and mid-chain hydroxy fatty acids; a critical review, Org. Geochem., 27, 1–13, 1997. doi.org/10.1016/S0146-6380(97)00063-6.

Versteegh, G.J.M., Jansen, J.H.F., De Leeuw, J.W. and Schneider, R.R.: Mid-chain diols and keto-ols in SE Atlantic sediments: a new tool for tracing past sea surface water masses? Geochim. Cosmochim. Ac. 64, 1879–1892, 2000. doi.org/10.1016/S0016-7037(99)00398-1.

Villanueva, L., Besseling, M., Rodrigo-Gámiz, M., Rampen, S.W., Verschuren, D. and Sinninghe Damsté, J.S. : Potential biological sources of long chain alkyl diols in a lacustrine system, Org. Geochem., 68, 27–30, 2014. doi.org/10.1016/j.orggeochem.2014.01.001.

Volkman, J.K., Barett, S.M. and Blackburn, S.I.: Eustigmatophyte microalgae are potential sources of C_{29} sterols, C_{22}–C_{28}n-alcohols and C_{28}–C_{32}n-alkyl diols in freshwater environments, Org. Geochem.,30, 307–318, 1999. doi.org/10.1016/S0146-6380(99)00009-1.

Walford, H.L., White, N.J. and Sydow, J.C.: Solid sediment load history of the Zambezi Delta, Earth Planet. Sc. Lett., 238 (1-2), 49-63, 2005. doi.org/10.1016/j.epsl.2005.07.014.

Wang, Y.V., Larsen, T., Leduc, G., Andersen, N., Blanz, T. and Schneider, R.R.: What does leaf wax δD from a mixed C_3/C_4 vegetation region tell us?, Geochem. Cosmochem. Ac., 111, 128-129, 2013. doi:10.10 16/j.gca.2012.10 .016.

Weijers, J.W.H., Schouten, S., van den Donker, J.C., Hopmans, E.C. and Sinninghe Damsté, J.S.: Environmental controls on bacterial tetraether membrane lipid distribution in soils, Geochim. Cosmochim. Ac., 71 pp. 703–713, 2007.

Weijers, J.W.H., Panoto, E., van Bleijswijk, J., Schouten, S., Rijpstra, W.I.C., Balk, M., Stams, A.J.M. and Sinninghe Damsté, J.S.: Constraints on the biological source(s) of the orphan branched tetraether membrane lipids, Geomicrobiol J., 26 402–414, 2009. doi.org.proxy.library.uu.nl/10.1080/01490450902937293.

Weldeab, S., Emeis, K.-C., Hemleben, C. and Siebel, W. : Provenance of lithogenic surface sediments and pathways of riverine suspended matter in the Eastern Mediterranean Sea: evidence from $^{143}Nd/^{144}Nd$ and $^{87}Sr/^{88}Sr$ ratios, Chem. Geol., 186, 139-149, 2002. doi.org/10.1016/S0009-2541(01)00415-6.

Weldeab, S., Lea, D.W., Oberhänsli, H. and Schneider, R.R.: Links between southwestern tropical Indian Ocean SST and precipitation over southeastern Africa over the last 17 kyr, Palaeo3., 140200-212, 2014. doi.org/10.1016/j.palaeo.2014.06.001.

Zhang, Z., Metzger, P. and Sachs, J.P., Co-occurrence of long chain diols, keto-ols, hydroxy acids and keto acids in recent sediments of Lake El Junco, Galapagos Islands Org. Geochem. 42, 823–837, 2011, doi: 10.1016/j.orggeochem.2011.04.012.

Zell, C., Kim, J.-H., Dorhout, D., Baas, M. and Sinninghe Damsté, J.S.S., Sources and distributions of branched tetraether lipids and crenarchaeol along the Portuguese continental margin: Implications for the BIT index, Cont. Shelf Res., 96, 34-44, 2015. doi.org/10.1016/j.csr.2015.01.006.

Figure Legend

Figure 1. Map presenting (a) the location of the core-tops (LOCO transect in orange, VA core-tops in blue) and cores (stars), (b) the mean annual salinity, from NOAA 1x1° grid (http://iridl.ldeo.columbia.edu), (c) the BIT index (LOCO transect values, VA core-tops from this study), (d) $F_{C32\ 1,15}$ in the core-tops, (e) #ring tetra of the surface sediments (#ring tetra as defined by Sinninghe Damsté, 2016), (f) Ternary diagram of C_{28} (sum of C_{28} 1,13 and C_{28} 1,14), C_{30} (sum of C_{30} 1,13, C_{30} 1,14 and C_{30} 1,15) and C_{32} (C_{32} 1,15) diols (LOCO transect in orange, VA core-tops in blue, data from Lattaud et al., 2017 in purple). The maps were drawn using Ocean Data View.

Figure 2. Organic and lithologic proxy records for core 64PE304-80 and parallel core GIK16160-3. (a) BIT index indicating soil and riverine input (Kasper et al., 2015) and $F_{C32\ 1,15}$ tracing riverine input (b) Red Sea Level changes (Grant et al., 2013) (c) log(Ca/Ti) indicating terrestrial input (van der Lubbe et al., 2013), (d) reconstruction of δD precipitation based on leaf wax *n*-C_{29} alkane of core GIK16160-3 (Wang et al., 2013), ε_{Nd} signatures of the clay fraction document changes in riverine influence (van der Lubbe et al., 2016). The grey bars show the Younger Dryas (YD) and Heinrich event 1 (H1) and 4 (H4). Black triangles indicate positions where ^{14}C AMS dates were obtained (Kasper et al., 2015)

Figure 3. Sources of riverine input in both area, (a) Location of core GeoB7702-3 (b) Close up location of core GeoB7702-3 (adapted from Castañeda et al., 2016) (c) source of the Nile river sediments (from Castañeda et al., 2016) and (d) Location of core 64PE304-80 and the Mozambique Channel (red circles shows source areas of the Zambezi river during dry conditions,

blue circle shows source area of the Zambezi river during wet conditions (Just et al., 2014), and green circle show northern rivers source area (van der Lubbe et al., 2016).

Figure 4. Organic and lithologic proxy records for core GeoB7702-3 and core 9509. (a) BIT index indicating soil and riverine input (Castañeda et al., 2010) and $F_{C32\ 1,15}$ tracing riverine input (b) Red Sea Level changes (Grant et al., 2013) (c) log(Ca/Ti) indicating terrestrial input (Castañeda et al., 2016), (d) reconstruction of δD precipitation based on leaf wax n-C_{31} alkane (Castañeda et al., 2016), (e) $^{87}Sr/^{86}Sr$ signatures of the sediment core 9509 (offshore the Israeli coast) document changes in riverine influence (Box et al., 2011). The grey bars show the sapropel layer (S1), Younger Dryas (YD), Heinrich event 1 (H1) and the Last Glacial Maximum (LGM). Black triangles indicate ^{14}C AMS dates (from Castañeda et al., 2010).

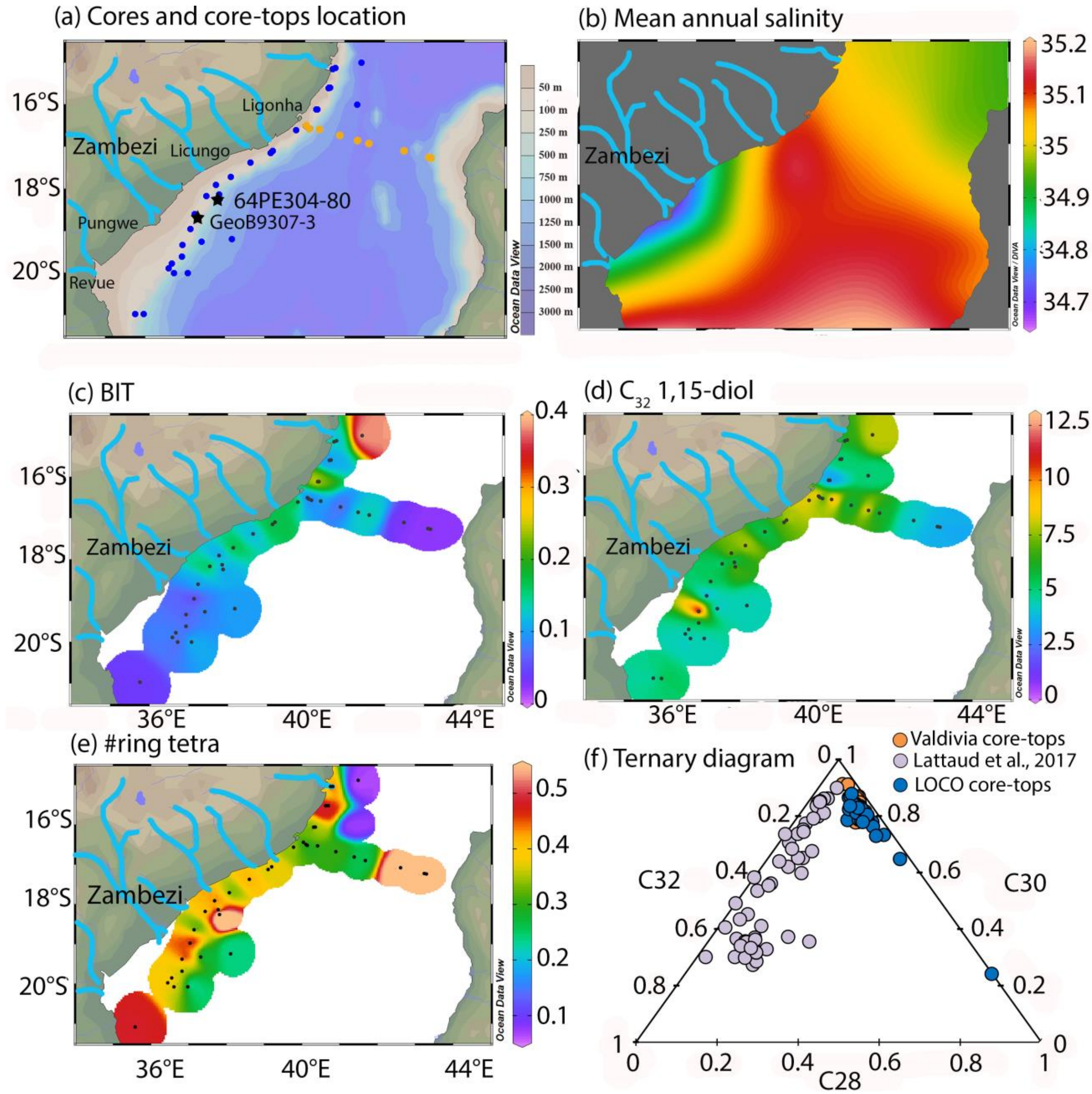
(a) Cores and core-tops location
16°S
18°S
20°S
Zambezi
Licungo
Ligonha
Pungwe
Revue
64PE304-80
GeoB9307-3
50 m
100 m
250 m
500 m
750 m
1000 m
1250 m
1500 m
2000 m
2500 m
3000 m
Ocean Data View
(b) Mean annual salinity
Zambezi
35.2
35.1
35
34.9
34.8
34.7
Ocean Data View / DIVA
(c) BIT
16°S
18°S
20°S
Zambezi
0.4
0.3
0.2
0.1
0
36°E
40°E
44°E
Ocean Data View
(d) C_{32} 1,15-diol
Zambezi
12.5
10
7.5
5
2.5
0
36°E
40°E
44°E
Ocean Data View
(e) #ring tetra
16°S
18°S
20°S
Zambezi
0.5
0.4
0.3
0.2
0.1
36°E
40°E
44°E
Ocean Data View
(f) Ternary diagram
Valdivia core-tops
Lattaud et al., 2017
LOCO core-tops
C32
C30
C28
0
0.2
0.4
0.6
0.8
1

Figure 1

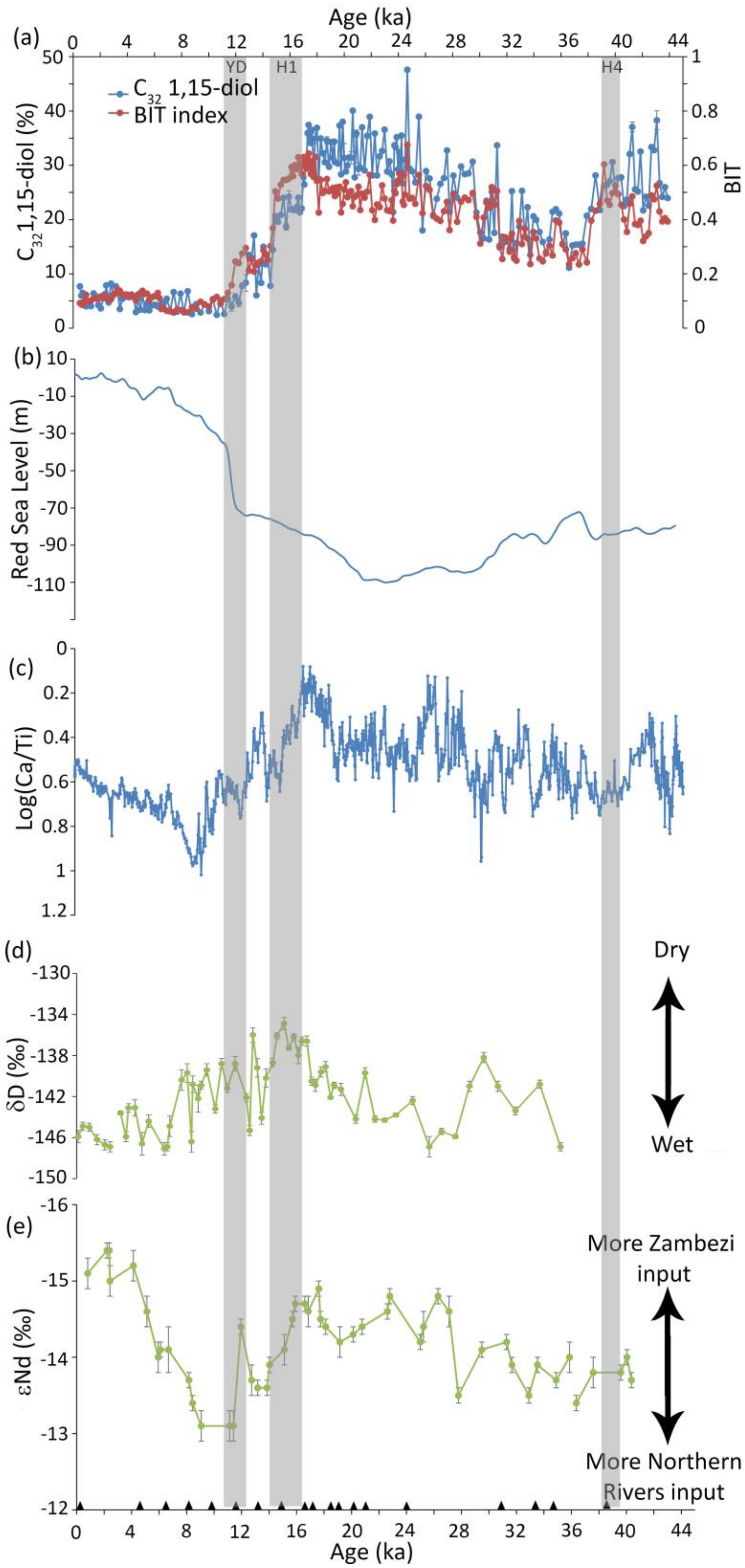

Age (ka)
(a)
(b)
(c)
(d)
(e)
YD
H1
H4
C32 1,15-diol
BIT index
C32 1,15-diol (%)
BIT
Red Sea Level (m)
Log(Ca/Ti)
δD (‰)
Dry
Wet
εNd (‰)
More Zambezi input
More Northern Rivers input

Figure 2

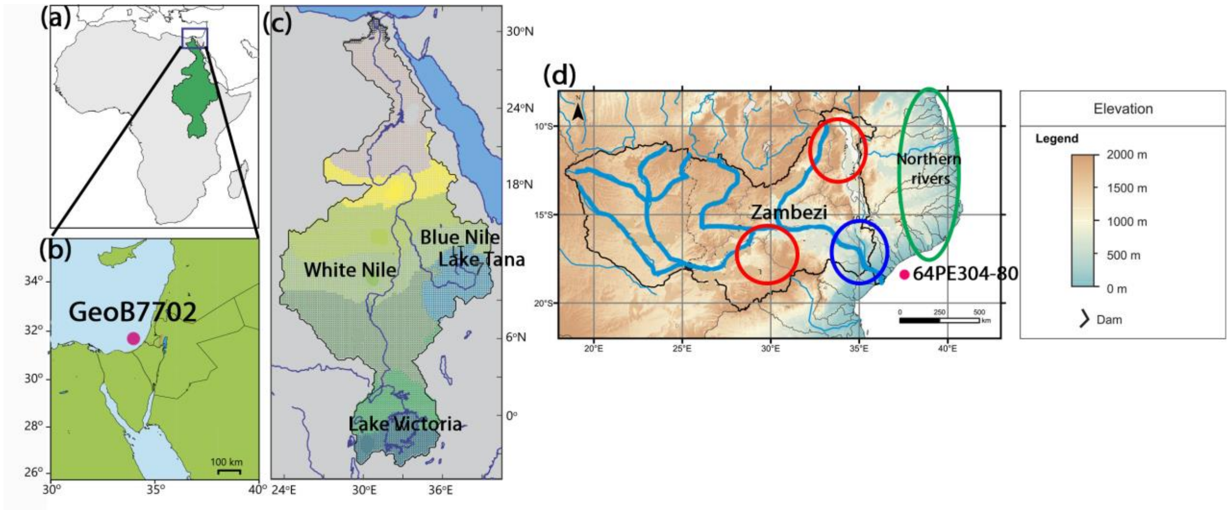

(a)
(b)
(c)
(d)
GeoB7702
100 km
34°
32°
30°
28°
26°
30°
35°
40°
White Nile
Blue Nile
Lake Tana
Lake Victoria
30°N
24°N
18°N
6°N
0°
24°E
30°E
36°E
Zambezi
Northern rivers
64PE304-80
10°S
15°S
20°S
20°E
25°E
30°E
35°E
40°E
Elevation
Legend
2000 m
1500 m
1000 m
500 m
0 m
Dam

Figure 3

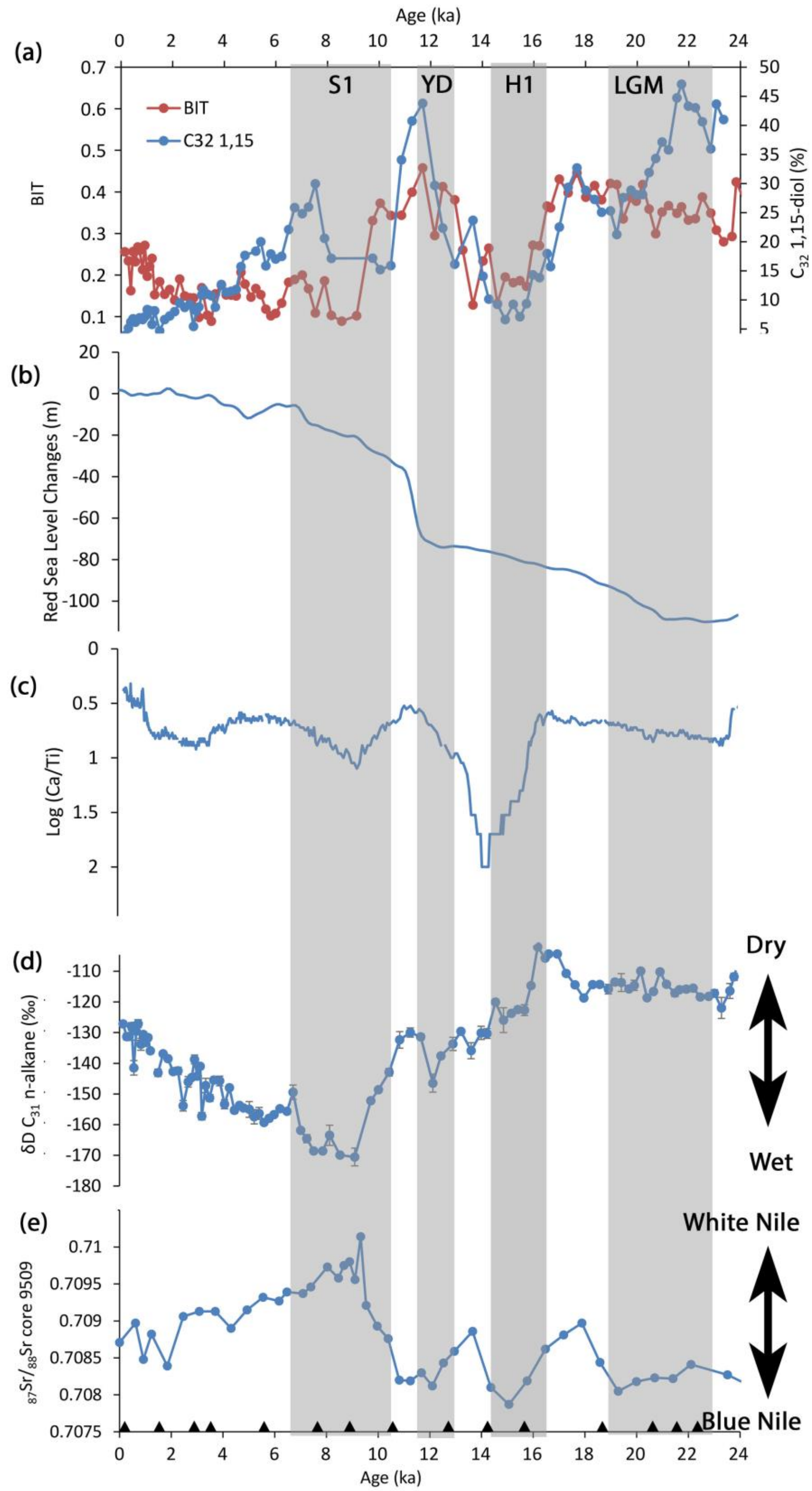
Age (ka)
(a)
S1
YD
H1
LGM
BIT
C32 1,15
BIT
C32 1,15-diol (%)
(b)
Red Sea Level Changes (m)
(c)
Log (Ca/Ti)
(d)
δD C31 n-alkane (‰)
Dry
Wet
(e)
87Sr/88Sr core 9509
White Nile
Blue Nile
Age (ka)

Figure 4